していることが知られており、老人斑と並ぶ AD 主病変である神経原線維変化の形成にもリン酸化の亢進が大きく関与していることが広く知られている。

そこで本研究では、加齢に伴うリン酸化・脱リン酸化バランスの異常が軸索輸送の障害を引き起こすのではないかと仮定し、神経系培養細胞を用いてリン酸化亢進による軸索輸送の障害を検索した。

B. 研究対象および方法

神経系培養細胞である Neuro2a 細胞にリン酸化亢進処理（オカダ酸処理）を施し、westernblot 法を用いた生化学的検索および免疫細胞化学的検索によって軸索輸送の障害を評価する。

＜生化学的検索＞

12 穴プレートに $2.0x10^4/cm^2$ の密度で Neuro2a 細胞を撒き、ITS-X サプリメント含有無血清培地にて 3 日間培養する。
軸索様の突起伸長が誘導されたことを確認した後、最終濃度が 100 および 200nM になるよう調整したオカダ酸を培地交換によって添加し、1 時間後に細胞を回収してライセート化したものを westernblot に用いた。

＜免疫細胞化学的検索＞

2 穴チェンバースライドに $1.0x10^4/cm^2$ の密度で Neuro2a 細胞を撒き、ITS-X サプリメント含有無血清培地にて 3 日間培養する。最終濃度が 200nM になるよう調整したオカダ酸を培地交換によって添加し、1 時間後に 4%PFA で固定して免疫染色に用いた。

C. 研究結果：

オカダ酸処理によって脱リン酸化酵素の活性が阻害された細胞では、dynein および dynactin に大きな変化はみられなかったが、late endosome のマーカーでもある Rab7 GTPase のタンパク量が有意に増加していた（Fig.1）。

免疫細胞化学的検索として、まず α-tubulin と Rab7 に対する抗体を用いて二重染色を行ったところ、Rab7 陽性エンドソームの肥大化が確認されたが、α-tubulin の陽性像には特に大きな変化は認められなかった。次に、dynein intermediate chain と P150dynactin に対する抗体を用いて二重染色を行ったところ、両者の共在性に変化は見られなかった（Fig.2）。

D. 考察：

本年度の研究成果の 1 つとして、dynein ノックダウンによる軸索輸送の機能障害はエンドサイトーシス障害を引き起こし、その結果として各種エンドソームの GTPase タンパク量増加ならびに肥大化病変が形成される可能性が示唆されている（研究代表者・木村）。そこで本研究では軸索輸送の加齢性障害メカニズムを明らかにするため、加齢によって生じると考えられているリン酸化・脱リン酸化バランスの障害との関係を検索したところ、リン酸化の亢進によって Rab7 GTPase タンパク量の増加とともにエンドソームの肥大化が確認され、エンドサイトーシス障害が生じていることが示唆された。α-tubulin の陽性像に大きな変化が認められなかったことから、今回の実験系で用いたオカダ酸の処理条件は微小管構造を破壊するものではなく、エンドサイトーシス障害もまた微小管構造の崩壊によって

生じているものではないことが確認された。一方、dynein intermediate chain と P150dynactin の共在性に明らかな変化が見られなかったことから、今回確認されたリン酸化亢進による軸索輸送の障害は dynein intermediate chain と dynactin との結合低下よりもむしろ、dynein heavy chain の ATPase 活性低下に大きく起因するものである可能性が示唆された。

E. 結論：

老齢脳ではリン酸化・脱リン酸化のバランスに障害が生じていること、そして AD 患者の脳組織では脱リン酸化酵素の活性が著しく低下していることから、リン酸化の亢進は加齢と AD 発症メカニズムを結びつける因子の一つであるとも考えられている。事実、AD 主病変の神経原線維変化は微小管結合蛋白 tau の異常リン酸化によって形成される病変であることからも、AD 病態におけるリン酸化・脱リン酸化バランス障害の関連性は非常に大きいと考えられる。

そして本研究の結果、リン酸化の亢進は軸索輸送障害によるものとほぼ同様のエンドサイトーシス障害を引き起こすことが明らかとなった。軸索輸送のモーター蛋白である dynein は、各サブユニットのリン酸化によってモーターとしての機能調節を受けていると考えられている。このことから、加齢に伴うリン酸化・脱リン酸化バランスの障害が、軸索輸送の加齢性低下・障害の原因の１つとなっている可能性が非常に高いと考えられる。

F. 健康危険情報

G. 研究発表

1. 論文発表

Takahashi M, Negishi T, Imamura M, Sawano E, Kuroda Y, Yoshikawa Y, Tashiro T.
Alterations in gene expression of glutamate receptors and exocytosis-related factors by a hydroxylated-polychlorinated biphenyl in the developing rat brain.
Toxicology. 257(1-2): 17-24. 2009.

Kobayashi Y, Negishi T, Mizumura A, Watanabe T, Hirano S. Distribution and excretion of arsenic in cynomolgus monkey following repeated administration of diphenylarsinic acid. ***Arch Toxicol***. 82(8): 553-61. 2008

2. 学会発表

小柳 洸志, 高橋 理貴, 根岸 隆之, 田代 朋子. 初代培養ラット小脳顆粒細胞における低カリウム誘発細胞死に対する内因性グルタミン酸の役割. 第51回日本神経化学会大会. 富山県. 2008年9月11-13日

若佐 美佳、今村 誠、吉岡 良祐、高橋 理貴、根岸 隆之、角田 正史、相澤 好治、田代 英夫、田代 朋子. トリブチルスズ経世代曝露による発達期脳の遺伝子発現変化. 第51回日本神経化学会大会. 富山県. 2008年9月11-13日

高橋 理貴、根岸 隆之、澤野 恵梨香、田代 朋子. LPS 誘導末梢性炎症による脳内甲状腺ホルモンシステムの変化. 第51回日本神経化学会大会. 富山県. 2008年9月11-13日

H. 知的財産権の出願・登録状況

なし

Fig. 1

A

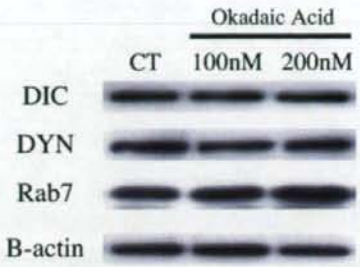

DIC: dynein intermediate chain
DYN: P150dynactin

B

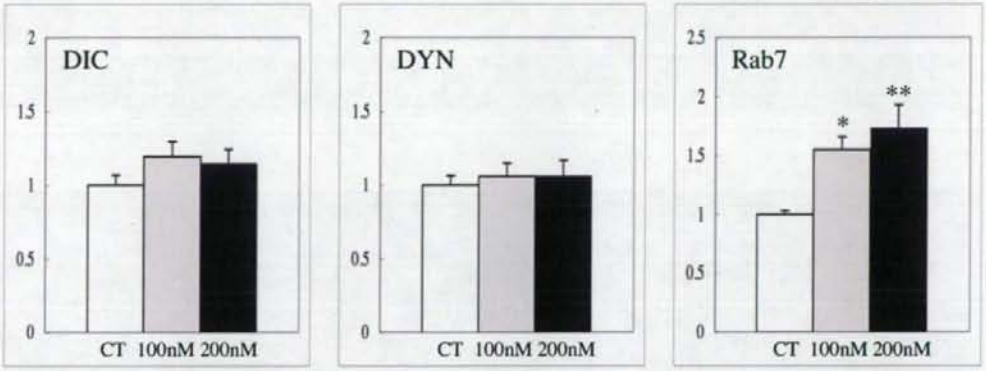

Fig. 2

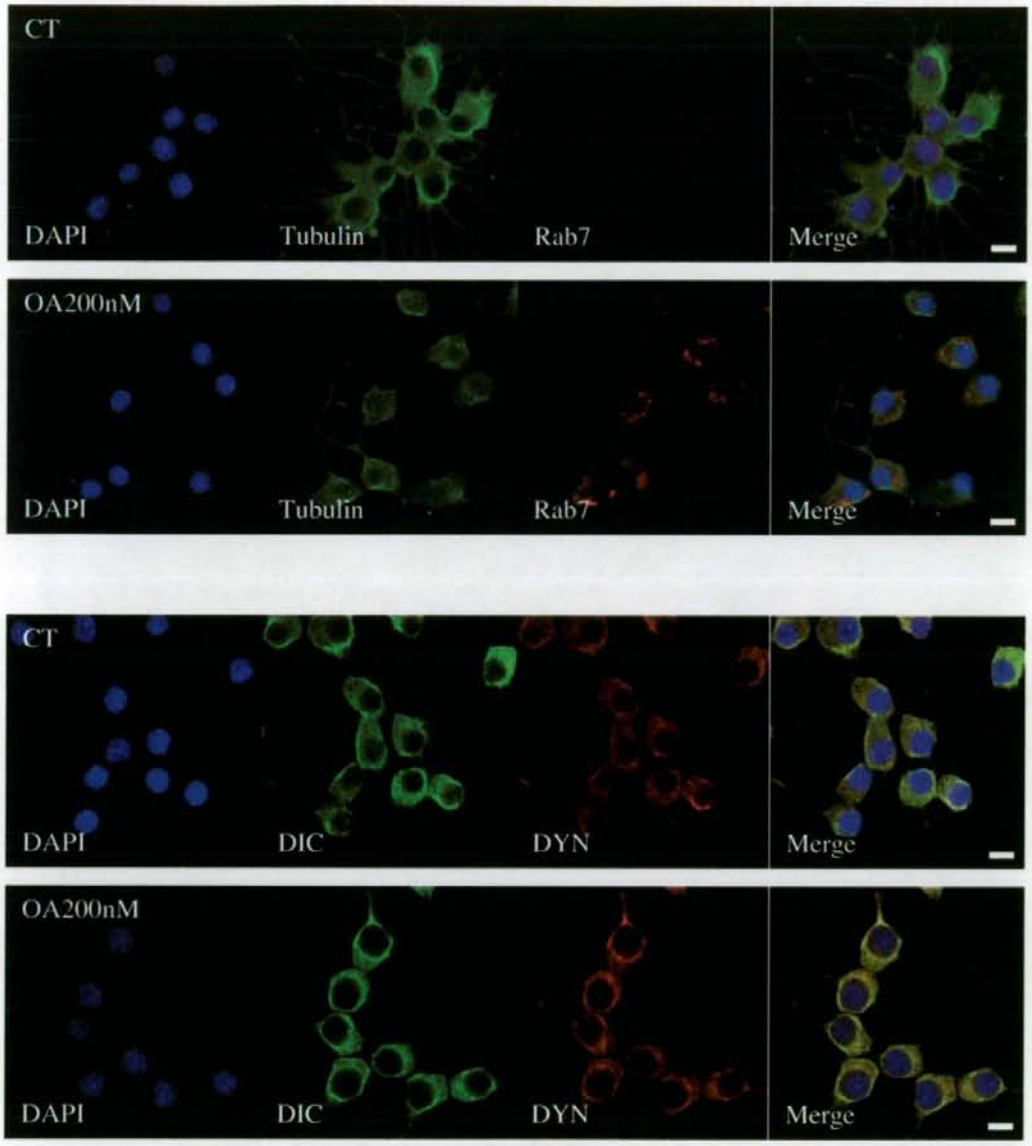

Scale Bar: 10μm

III. 研究成果の刊行に関する一覧表

研究成果の刊行に関する一覧表

雑誌

発表者氏名	論文タイトル名	発表誌名	巻号	ページ	出版年
Okabayashi S and Kimura N.	Leucine-rich glioma inactivated 3 is involved in amyloid β peptide uptake by astrocytes and endocytosis itself.	Neuroreport.	19(12)	1175-1179	2008
Kobayashi Y, Negishi T, Mizumura A, Watanabe T, Hirano S.	Distribution and excretion of arsenic in cynomolgus monkey following repeated administration of diphenylarsinic acid.	Arch Toxicol	82(8):	553-561.	2008
Takahashi M, Negishi T, Imamura M, Sawano E, Kuroda Y, Yoshikawa Y, Tashiro T.	Alterations in gene expression of glutamate receptors and exocytosis-related factors by a hydroxylated-polychlorinated biphenyl in the developing rat brain.	Toxicology	257(1-2):	17-24	2009

Leucine-rich glioma inactivated 3 is involved in amyloid β peptide uptake by astrocytes and endocytosis itself

Sachi Okabayashi[a,b] and Nobuyuki Kimura[a]

[a]Laboratory of Disease Control, Tsukuba Primate Research Center, National Institute of Biomedical Innovation and [b]The Corporation for Production and Research of Laboratory Primates, 1-1 Hachimandai, Tsukuba-shi, Ibaraki, Japan

Correspondence to Nobuyuki Kimura, Laboratory of Disease Control, Tsukuba Primate Research Center, National Institute of Biomedical Innovation, 1-1 Hachimandai, Tsukuba-shi, Ibaraki 305-0843, Japan
Tel: +81 29 837 2121; fax: +81 29 837 0218; e-mail: kimura@nibio.go.jp

Received 23 May 2008; accepted 26 May 2008

We earlier showed that leucine-rich glioma inactivated 3 (LGI3) co-localizes with amyloid β peptide (Aβ) taken up by astrocytes both *in vitro* and *in vivo*, and that LGI3 accumulated with endocytosis-associated proteins in aged monkey brains. In this study, we confirmed that LGI3 localizes to the endocytic pathway and found that its accumulation is caused by endocytic perturbation. Most notably, RNA interference experiments demonstrated that the down-regulation of LGI3 clearly inhibited Aβ uptake by cultured rat astrocytes, moreover, transferrin uptake by both astrocytes and neuronal cells. Together with our earlier findings, our results suggest that LGI3 is involved in Aβ uptake by astrocytes and even endocytosis itself. *NeuroReport* 19:1175–1179 © 2008 Wolters Kluwer Health | Lippincott Williams & Wilkins.

Keywords: Alzheimer's disease, amyloid beta-protein, endocytosis, leucine-rich glioma inactivated 3

Introduction

Amyloid β protein (Aβ) is the major component of senile plaques, a characteristic feature of Alzheimer's disease [1–4], and astrocytes are considered to have an important role in clearing Aβ from the brain [5–7]. We have recently demonstrated that Aβ upregulates and colocalizes with leucine-rich glioma inactivated 3 (LGI3), a transmembrane protein containing leucine-rich repeat domains, in cultured rat astrocytes [8] and that LGI3 accumulates in a granular manner with endocytosis-associated proteins and lipid raft markers in aged monkey brains [9]. These findings led us to hypothesize that LGI3 might be involved in astroglial response against Aβ via endocytosis system, that is, Aβ uptake by astrocytes, however, the function of LGI3 in the brain remains unknown.

In this study, we carried out immunocytochemical and biochemical analyses to investigate whether LGI3 localizes to the endocytic pathway. We also conducted RNA interference experiments to test our hypothesis that LGI3 may be involved in Aβ uptake by astrocytes and endocytosis in neural cells.

Materials and methods

Cell cultures

Rat astrocyte cultures were prepared as described before [8]. Briefly, cerebral cortical cultures were prepared from embryonic day 18 Sprague–Dawley rats (SLC Japan, Shizuoka, Japan) and cultured in culture medium (CM, Dulbecco's modified eagle's medium with 10% fetal calf serum). After 14 days of culturing, cerebral cortical cells were dissociated with 0.025% trypsin and washed several times in CM. By means of this procedure, proliferating type-1 astrocytes were quickly selected from the cell suspension [10]. For western blot analyses, cells were plated at 2.0×10^4 cells/cm^2 onto six-well plates coated with collagen type I (Greiner bio-one, Heidelberg, Germany). For immunocytochemical studies, cells were plated at 1.0×10^4 cells/cm^2 onto 2-well LAB-TEK chamber slides (Nalge Nunc, Rochester, New York, USA) coated with 5 μg/cm^2 collagen type I (BD Bioscience, Bedford, Massachusetts, USA). All animal experiments were carried out according to the National Institute of Biomedical Innovation rules and guidelines for experimental animal welfare.

Neuronal cell line, mouse neuroblastoma Neuro2a, is a kind gift from Dr Yoshida and Dr Yokota, Tokyo Medical and Dental University. Neuro2a cells were cultured in CM, and plated at 1.5×10^4 cells/cm^2 onto 6-well plates coated with 0.01% poly-L-lysine (Wako, Osaka, Japan) for western blot analyses.

Drug treatments

Cells were treated with the following drugs at the indicated final concentrations: chloroquine (200 and 500 nM) and NH_4Cl (2 and 5 mM); both were purchased from Wako.

RNA interference, amyloid β peptide, and transferrin treatments

For double-stranded RNA-mediated interference (RNAi) studies, we used the following short double-stranded RNA (siRNA) against LGI3: siRNA-1, 5′-GCACCCGGUGUC

CAUCUAUAA-3′(sense) and 5′-AUAGAUGGACACCGG GUGCAG-3′(antisense); siRNA-2, 5′-GAAAUUUGUACG GUUCCAAGA-3′(sense) and 5′-UUGGAACCGUACAA AUUUCUG-3′(antisense). The control siRNA had a random sequence. RNAi experiments were carried out by using siLentFect lipid reagent (BioRad, Hercules, California, USA), according to the manufacturer's protocol. Seventy-two hours after siRNA transfection, cells were treated with either Aβ or transferrin at the indicated final concentrations: 1 μM Aβ1-40 peptides for western blotting and 100 nM for immunocytochemistry (Aβ40 was not preaggregated; Peptide, Osaka, Japan); and 100 nM biotin-conjugated human transferrin for western blotting and 50 nM for immunocytochemistry (SIGMA, St Louis, Missouri, USA).

Immunocytochemistry

Cells plated on chamber slides were fixed with 4% paraformaldehyde and then permeabilized with 0.01 or 0.1% Triton X-100 for 5 min at room temperature. After blocking with 3% bovine serum albumin, cells were incubated for 1 h at room temperature with the following primary antibodies: rabbit polyclonal anti-LGI3; [8] mouse monoclonal anti-Rab5 (Santa Cruz Biotechnology, Santa Cruz, California, USA); and mouse monoclonal anti-Aβ40 (IBL, Gunma, Japan). Cells were then incubated with AlexaFluor 555-conjugated anti-rabbit IgG and either AlexaFluor 488-conjugated anti-mouse IgG or AlexaFluor 488-conjugated streptavidin (Invitrogen), followed by 4′-6-Diamidino-2-phenylindole nuclear stain (Santa Cruz Biotechnology) for 1 h at room temperature. All cells were examined with a Digital Eclipse C1 confocal microscope (NIKON, Kanagawa, Japan). We performed three independent experiments.

Western blot analyses

Cells were harvested in PBS and centrifuged to obtain cell pellets. The pellets were lysed in a solution containing 62.5 mM Tris–HCl (pH 6.8), 2 mM EDTA, 0.5% Triton X-100, 2% SDS, and Complete Mini proteinase inhibitor cocktail (Roche Molecular Biochemicals, Penzberg, Germany) to extract total cellular proteins. Total proteins were adjusted to 10 μg and then subjected to SDS-polyacrylamide gel electrophoresis with 10 or 15% acrylamide gels. Separated proteins were blotted onto nitrocellulose membranes (Aβ) or polyvinylidene fluoride membranes (other proteins). Blotted nitrocellulose membranes were heated in boiling PBS for 5 min to enhance the signal [11]. The membranes were blocked with 5% nonfat dried milk in PBS containing 0.1% Tween-20, then incubated for 1 h at room temperature with the following primary antibodies: rabbit polyclonal anti-LGI3; mouse monoclonal anti-β-actin (SIGMA); rabbit polyclonal anti-GFAP (DAKO, Glostrup, Denmark); mouse monoclonal anti-Rab5; mouse monoclonal anti-Aβ40; and goat polyclonal anti-transferrin (BETHYL, Montgomery, Texas, USA). They were then incubated with horseradish peroxidase-conjugated secondary antibodies (Jackson Immunoresearch Laboratories, West Grove, Pennsylvania, USA) for 1 h at room temperature. Immunoreactive elements were visualized via enhanced chemiluminescence (ECLplus, GE Healthcare, Buckinghamshire, UK). For the transferrin treatment study, we also examined horseradish peroxidase-conjugated streptavidin (DAKO) to detect biotin-conjugated transferrin taken up by cells. We carried out three independent experiments (N=6 for each experimental group), duplicating each experiment.

Data analyses

To confirm the reproducibility of our results, we quantified immunoreactive bands obtained from the western blots with commercially available software (Quantity One; PDI, Inc., Upper Saddle River, New Jersey, USA). Data are shown as means ± SD. For statistical analyses, one-way analysis of variances were carried out followed by the Bonferroni/Dunn post-hoc test.

Results

Leucine-rich glioma inactivated 3 localizes to the endocytic pathway and accumulates with drug treatments

First of all, we carried out immunocytochemistry to assess whether LGI3 localized to the endocytic pathway. Under mild permeabilization conditions (0.01% Triton X-100), LGI3 colocalized with Rab5, an early endosome marker, in cultured rat astrocytes (Fig. 1a). Under ordinary permeabilization conditions (0.1% Triton X-100), however, LGI3 mainly localized to plasma membranes and nuclei, as described before (data not shown) [8].

Chloroquine and NH_4Cl are drugs well-known to perturb membrane trafficking from endosomes to lysosomes. After a 1-h drug treatment, LGI3 clearly accumulated in enlarged early endosomes, even the case in cells treated with NH_4Cl, which is less potent than chloroquine (Fig. 1a). Western blot analyses also demonstrated that endocytic perturbation caused LGI3 accumulation in cultured rat astrocytes in a dose-dependent manner (Fig. 1b, c). By means of over-exposure, we observed LGI3-mid and LGI3-low, two possible byproducts of LGI3 cleavage [9] (Fig. 1b).

Leucine-rich glioma inactivated 3 is involved in endocytosis in both astrocytes and neuronal cells

We designed two LGI3-specific siRNAs and tested their ability to downregulate LGI3 in cells. Western blot analyses revealed that siRNA-1 most potently downregulated LGI3 (Fig. 2a, b); siRNA-2 also downregulated LGI3 significantly (data not shown).

Noteworthy, western blot analyses demonstrated that the downregulation of LGI3 clearly inhibited Aβ uptake in cultured rat astrocytes (Fig. 2a, b). Immunocytochemistry also confirmed that Aβ was hardly taken up by LGI3-immunonegative cells (Fig. 2c). Quite interestingly, the downregulation of LGI3 also significantly inhibited transferrin uptake by cultured rat astrocytes (Fig. 2a, b). Immunocytochemistry demonstrated that LGI3 colocalized with transferrin taken up by cells transfected with control siRNA (Fig. 2c), however, transferrin immunoreactivity diminished in LGI3-downregulated cells (Fig. 2c). This was also the case in cells transfected with siRNA-2 (data not shown).

To assess whether LGI3 is also involved in endocytosis in neuronal cells as well as astrocytes, we examined another siRNA study by using neuronal cell line, Neuro2a. Noteworthy, the downregulation of LGI3 also significantly decreased transferrin uptake by Neuro2a cells (Fig. 3).

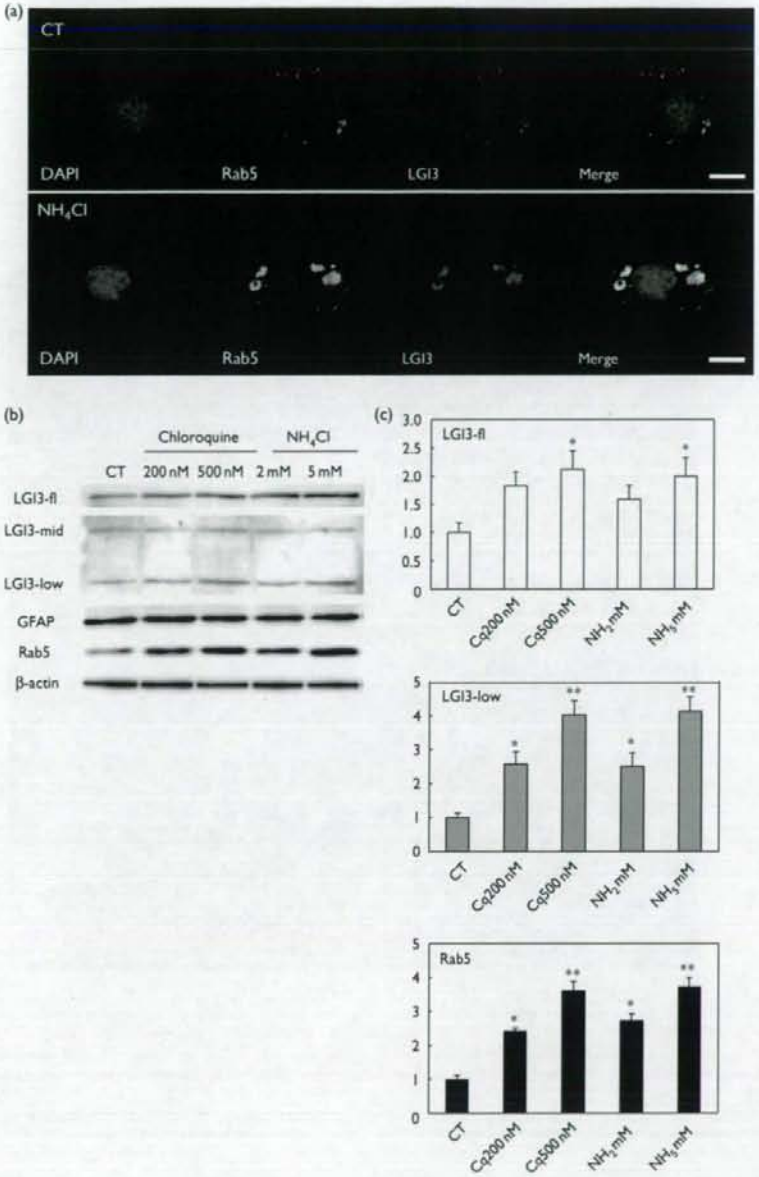

Fig. 1 (a) Photomicrographs of cultured rat astrocytes. Owing to the mild permeabilization method used, we were able to observe that leucine-rich glioma inactivated 3 (LGI3) was localized to Rab5-positive early endosomes. NH_4Cl treatment induced enlargement of early endosomes, where LGI3 clearly accumulated. Scale bars, 10 μm. (b) Western blots showing the amount of LGI3, GFAP, Rab5, and β-actin in cultured rat astrocytes treated with drugs. Drug treatments induced accumulation of LGI3 and Rab5; however, the amount of GFAP and β-actin remained unchanged. Overexposure revealed that LGI3-low, one of the byproducts of LGI3, clearly accumulated in cells treated with drugs. (c) Histograms showing the effect of drug treatments on the amount of full-length LGI3 (LGI3-fl), LGI3-low, and Rab5. All data were normalized according to β-actin levels (CT, control). Values are means ± SD. $^*P < 0.05$; $^{**}P < 0.01$. CT, control; Cq, cells treated with chloroquine; NH, cells treated with NH_4Cl. Y-axes show the mean values of the quantified data.

Discussion

LGI3 colocalized with the early endosome marker Rab5, and drug-induced endocytic perturbation caused LGI3 to accumulate in enlarged early endosomes (Fig. 1a). These findings suggest that LGI3 really localizes to the endocytic pathway of neural cells and supports our earlier finding that LGI3 colocalizes with endocytosis-associated proteins in monkey brains [9]. Western blot analyses also confirmed that endocytic perturbation caused LGI3 to accumulate in cells (Fig. 1b, c), suggesting that LGI3 accumulation in aged

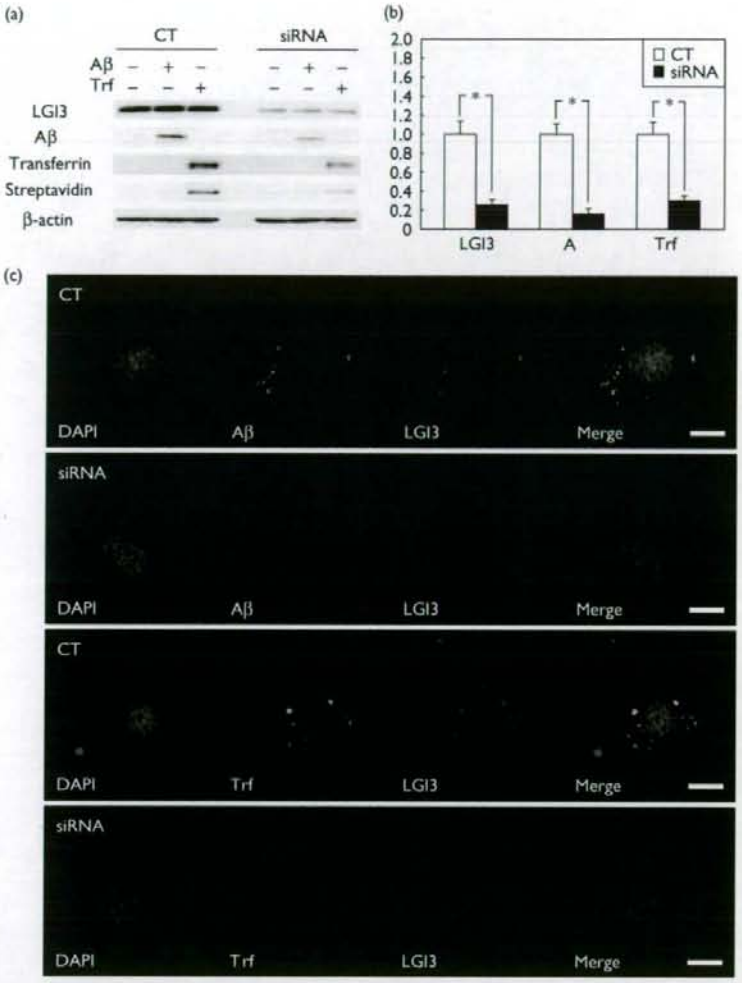

Fig. 2 (a) Western blots showing the amount of leucine-rich glioma inactivated 3 (LGI3) and the uptake levels of amyloid β peptide (Aβ) and transferrin (Trf) in cultured rat astrocytes 72 h after treatment with siRNA-1. In cells transfected with siRNA-1, LGI3 was clearly downregulated, and the uptake levels of Aβ and transferrin apparently decreased. (b) Histograms showing the effect of siRNA-1 transfection on the amount of LGI3-fl and on the uptake levels of Aβ and transferrin in cultured rat astrocytes. All data were normalized according to β-actin protein levels (CT, control). Values are means ± SD. $^*P < 0.001$. CT, cells transfected with control siRNA; siRNA, cells transfected with siRNA-1. Y-axes show the mean values of the quantified data. (c) Photomicrographs of cultured rat astrocytes. LGI3-immunonegative cells took up very little, if any, Aβ. In control cells, LGI3 colocalized with Aβ. Although LGI3 also colocalized with transferrin in control cells, transferrin immunoreactivity, which reflects the transferrin taken up by cells, diminished in LGI3-downregulated cells. CT, cells transfected with control siRNA; siRNA, cells transfected with siRNA-1.

monkey brains [9] likely may be caused by age-dependent disturbances in the endocytosis system. As chloroquine and NH_4Cl treatments blocked lysosomal degradation, the finding that accumulation of LGI3-low after endocytic perturbation also suggests that LGI3 and/or its byproducts may be degraded by lysosomes.

We earlier showed that Aβ treatment induced the upregulation of LGI3 in cultured rat astrocytes, and LGI3 colocalized with Aβ taken up by astrocytes both *in vitro* and *in vivo* [8,9]. In this study, RNAi experiments revealed that siRNA-induced downregulation of LGI3 significantly decreased Aβ uptake by cultured rat astrocytes (Fig. 2). This is the first study to show that LGI3 is involved in Aβ uptake by astrocytes. We also examined transferrin uptake to assess whether LGI3 mediates Aβ-specific uptake in astrocytes. Notably, the downregulation of LGI3 significantly decreased transferrin uptake by cultured rat astrocytes, and LGI3 colocalized with the internalized transferrin (Fig. 2).

Transferrin is a well-known marker for clathrin-dependent endocytosis. How Aβ is taken up by glial cells, however, remains controversial. A recent study showed that Aβ internalization is independent of clathrin but dependent on dynamin and cellular lipids, suggesting that Aβ uptake may be mediated by an endocytic pathway involving caveolae/lipid rafts [12]. As we earlier showed

Arch Toxicol (2008) 82:553–561
DOI 10.1007/s00204-007-0270-x

INORGANIC COMPOUNDS

Distribution and excretion of arsenic in cynomolgus monkey following repeated administration of diphenylarsinic acid

Yayoi Kobayashi · Takayuki Negishi · Ayano Mizumura · Takayuki Watanabe · Seishiro Hirano

Received: 14 September 2007 / Accepted: 28 November 2007 / Published online: 19 December 2007

Abstract Diphenylarsinic acid (DPAA), a possible product of degradation of arsenic-containing chemical weapons, was detected in well water in Kamisu City, Ibaraki Prefecture, Japan, in 2003. Although some individuals in this area have been affected by drinking DPAA-containing water, toxicological findings on DPAA are limited. To elucidate the mechanism of its toxicity, it is necessary to determine the metabolic behavior of DPAA in the body. In this study, pregnant cynomolgus monkeys at the 50th day of pregnancy were used. The monkeys were treated daily with 1.0 mg DPAA/kg body weight using a nasogastric tube, and the distribution and excretion of arsenic were examined after the repeated administration and 198–237 days after the last administration of DPAA. Fecal excretion was higher than urinary excretion (ca. 3:2 ratio), and arsenic accumulated in the hair and erythrocytes. Distribution of DAPP to plasma and hemolyzed erythrocytes was also examined by high-performance liquid chromatography–inductively coupled argon plasma mass spectrometry (HPLC–ICP MS). Two peaks were found in the elution profile of arsenic, due to free and probably protein-bound DPAA. The protein-bound arsenic compounds were presumably trivalent diphenylarsenic compounds, since free DPAA was recovered after treatment of heat-denatured samples with hydrogen peroxide.

Keywords Diphenylarsinic acid (DPAA) · Monkey · Arsenic speciation · Distribution · Excretion · HPLC–ICP MS

Y. Kobayashi (✉)
Environmental Health Sciences Division,
National Institute for Environmental Studies,
16-2 Onogawa, Tsukuba, Ibaraki 305-8506, Japan
e-mail: kobayashi.yayoi@nies.go.jp

T. Negishi
Department of Chemistry and Biological Science,
Aoyama Gakuin University, 4-4-25 Shibuya,
Shibuyaku, Tokyo 150-8366, Japan

A. Mizumura · T. Watanabe · S. Hirano
Graduate School of Pharmaceutical Sciences,
Chiba University, 1-8-1 Inohana, Chuo-ku,
Chiba 260-8675, Japan

S. Hirano
Research Center for Environmental Risk,
National Institute for Environmental Studies,
16-2 Onogawa, Tsukuba, Ibaraki 305-8506, Japan

Introduction

Clark 1 (diphenylarsine chloride) and Clark 2 (diphenylarsine cyanide), which are sternutators, and Lewisite (2-chloro-ethenyl dichloroarsine), a blister agent, were produced as chemical weapon agents (CWAs) during World War II. Environmental pollution caused by these chemicals has become a matter of public concern. In spring 2003, contamination of groundwater and soil by organic arsenic compounds such as diphenylarsinic acid (DPAA), bis (diphenylarsine) oxide, and phenylarsonic acid (PAA) were found in Kamisu Town (now Kamisu City), Ibaraki Prefecture, Japan (Ishii et al. 2004), and DPAA accounted for a large proportion of the detected organic arsenic compounds. The highest concentration of DPAA in the well water of Kamisu area was estimated to be around 4.5 mg As/l (Kinoshita et al. 2005; Shibata et al. 2005). Thus, a maximum daily intake of DPAA is supposed to have been 0.18 mg As/(kg day), assuming the body weight was 50 kg and the water consumption was 2 l/day. These chemicals were assumed to be products of degradation or

intermediate materials for the production of Clark 1 and Clark 2.

The toxicity of CWA-related organic arsenic compounds was confirmed in rat heart microvessel endothelial (RHMVE) cells (Hirano et al. 2005), HepG2 cells (Ochi et al. 2004, 2006), and other types of cells. Ochi et al. (2004) noted that DPAA exhibited cytotoxic effects on HepG2 cells at concentrations above 0.5 mM. DPAA induced structural and numerical chromosomal abnormalities, and triggered centrosome abnormalities or spindle abnormalities specific to cytokinesis. Ishii et al. (2004) reported that individuals who had been exposed to DPAA exhibited cerebellar symptoms, tremor, myoclonus, visual abnormalities, and disturbance of memorization as clinical manifestations. However, in vivo toxicological findings on DPAA are limited. Determination of the mechanism of toxicity of DPAA will require examination of its absorption, distribution, metabolism, and excretion. Although animal experiments often use rodents, sensitivity to arsenicals, distribution and metabolism of them in the body vary in a number of respects among mammals (Aposhian 1997). Studies in primates are more likely to yield accurate predictions of metabolism of DPAA in humans.

The present study focused on the metabolic behavior of DPAA, and involved measurement of arsenic levels in the blood, urine, feces, and hair of cynomolgus monkeys following repeated administration of DPAA. We also performed speciation analyses of DPAA in urine and blood by high-performance liquid chromatography–inductively coupled argon plasma mass spectrometry (HPLC–ICP MS) using a polymer-based gel filtration column.

Materials and methods

Chemicals

Diphenylarsinic acid, produced by Tri Chemicals (Yamanashi, Japan), was provided by the Japan Science Foundation. The purity of DPAA was >99%. Arsenobetaine [$(CH_3)_3AsCH_2COO$; AsB: 98%], Monomethylarsonic acid [$(CH_3)AsO(OH)_2$; MMA^V: 98%], and dimethylarsinic acid [$(CH_3)_2AsO(OH)$; DMA^V: 98%] were purchased from Tri Chemicals. For chemical analyses, stock solutions (100 μg As/ml) were prepared from each arsenic compound and stored at 4°C in the dark. Working standard solutions (10 ng As/ml) were prepared daily using Milli-Q SP water (Yamato Millipore, Japan). An arsenic standard solution (1,013 μg As/ml: Merck, Darmstadt, Germany) was used for total arsenic analysis. The following analytical-grade chemicals were purchased from Wako Pure Chemical Industries (Osaka, Japan): nitric acid, hydrogen peroxide, and ammonium acetate.

Animals

The present experiments were designed to investigate effects of in utero exposure to DPAA on neurological development. The administration of DPAA to animals and material sampling were performed at Shin Nippon Biomedical Laboratories, Ltd. (Kagoshima, Japan). These experiments were conducted in accordance with the Basic Policies for the Conduct of Animal Experimentation, provided by the Science Council of Japan (http://www.scj.go.jp/ja/info/kohyo/pdf/kohyo-20-k16-2e.pdf). Female cynomolgus monkeys (weight 3–4 kg) were purchased from the Guangxi Research Center of Primate Laboratory Animal (Nanning, Guangxi, China). Sixteen female monkeys (eight each for the control and DPAA group) were mated until the pregnancy was confirmed. All pregnant animals survived during the experimental period. Five control and six DPAA-administered animals delivered normally after the usual pregnant term (147–170 days). The blood, hair, and excreta samples were collected from three control and six DPAA-administered animals for the current study. The experimental protocol is shown Fig. 1. From the 50th day of pregnancy, nasogastric intubation was performed after restraint. DPAA was dissolved at a concentration of 0.2 mg DPAA/ml in pyrogen-free water and given at a dose of 1.0 mg DPAA/(kg day) [0.28 mg As/(kg day)] until delivery (98–121 days) through the nasogastric tube (twice a day; 6 h after the first administration, the same dose was given again) (DPAA group, $n = 6$). Vehicle water was given in similar fashion to a control group ($n = 3$). Blood was collected on Days 41–92, and urine, feces and hair samples were collected on Days 64–92 during administration. Heparinized blood was collected just before and 1 and 4 h after the first administration of DPAA on blood collection days (Days 41–92). An aliquot of the whole blood was separated into cellular and plasma fractions. The cells were washed 3 times in 50 mM Tris-buffered saline (pH 7.4, 25°C). After being mixed with 10 mM ammonium acetate solution, the samples were centrifuged at 15,000*g* for 30 min to prepare 20% erythrocyte lysate. Urine and feces were collected in a metabolic cage on the same day. Urine was collected over 24 h (on Days 64–92), and suspended solids were eliminated by centrifugation. Feces were collected separately from 0 to 6 h and from 6 to 24 h after the first administration. Dorsal hair was collected by cutting at about 2 mm above the skin using a clipper (on Days 64–92). Blood, plasma, 6-h urine, and 6-h fecal excretion were also collected (recovery group, $n = 6$) 198–237 days after delivery (after repeated administration had been terminated).

Analysis of arsenic

The feces were dried with a lyophilizer (FZ-2.5CSCL; LABOCONCO, MO, USA) and powdered with a mortar,

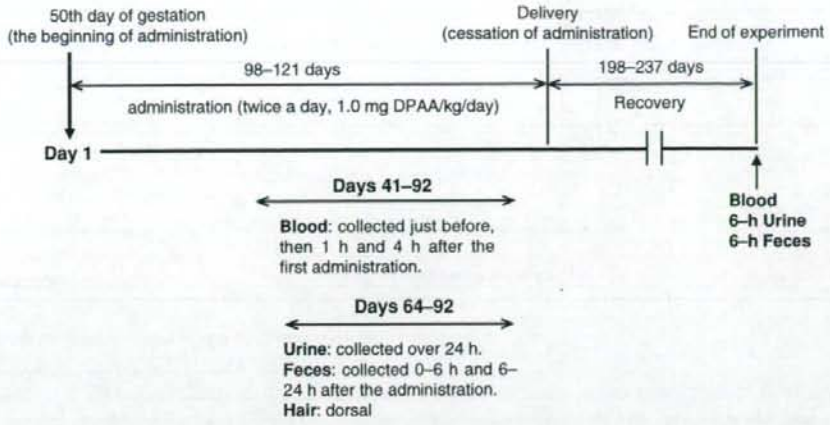

Fig. 1 Experimental protocol of the present study. Blood samples were collected on Days 41–92 (46, 64, and 72 days for the control group, and 41, 45, 48, 63, and 92 days for the DPAA group after the first administration). Urine, fecal, and hair samples were collected on Days 64–92 (64, 72, and 79 days for the control group, and 72, 76, 79, 85, and 92 days for the DPAA group after the first administration). Samples from the recovery group were collected at 198, 202, 209, 221, 233, and 237 days after cessation of administration

and a portion of the powder was weighed for measurement of arsenic concentration. The collected hair was cleaned by ultrasonication in 1% SDS solution for 20 min. After rinsing in ultrapure water three times, it was ultrasonically cleaned for 10 min twice, and then finally rinsed in ultrapure water. After drying at 50°C for 3 h, it was stored in a desiccator (Shraim et al. 2003). Whole blood, plasma, hair, urine, and feces were wet-ashed with nitric acid and hydrogen peroxide [3:1 (v:v)] and then measured by ICP MS (HP 7500; Yokogawa Analytical Systems, Musashino, Japan). Arsenic distribution in blood was calculated based on the assumption that whole blood accounts for 6.5% of an animal's weight. The amount of arsenic in blood cells was calculated based on the hematocrit (39.3 ± 3.8%) (Yoshida and Fujimoto 2006) of nonpregnant female cynomolgus monkeys.

Speciation analysis of protein-bound arsenic compounds

Aliquots of 300 µl of plasma and erythrocyte lysate were treated in boiling water for 10 min. After centrifugation at 15,000*g* for 30 min, the pellet was washed with PBS 3 times and reacted with 150 µl of 30% hydrogen peroxide at room temperature for 3 h to extract protein-bound arsenicals into a soluble fraction. After the addition of excess catalase (5,000 U), the supernatant was reacted at 37°C for 30 min to eliminate hydrogen peroxide from the sample. Speciation of arsenic was performed by HPLC–ICP MS. An aliquot of sample (20 µl) was applied to a gel filtration column, which was eluted with prefiltered (0.22 µm) mobile phase (50 mM ammonium acetate) at a flow rate of 0.5 ml/min. The HPLC system (Shimadzu, Kyoto, Japan) consisted of a CTO-20AC column oven, an LC-20AD solvent delivery module, a DGU-20A_3 degasser, a 7125 six-port injection valve with a 20-µl injection loop (Rheodyne, CA, USA), and a polymer-based gel filtration column (Shodex Asahipak GS–220HQ; 300 mm × ø 7.6 mm i.d.; exclusion limit > 3,000; Showa Denko, Japan). The eluent was introduced directly into the nebulizer of the ICP MS to detect arsenic. Signal intensities at *m/z* 75, 35, and 77 were monitored for As, Cl, and ArCl, respectively.

Stability of protein-bound arsenic compounds in erythrocyte lysate

Erythrocyte lysate was obtained on Days 41–92. To examine the stability of protein-bound arsenic compounds, erythrocyte lysate was incubated at 37°C for 0–24 h for analysis of arsenic chemical species by HPLC–ICP MS.

Validation methods

The detection limit (DL) for total arsenic was 0.02 ng As/ml with ICP MS (*m/z* 75 for As). The DLs ($s/n = 3$) for MMA^V, DMA^V, AsB, and DPAA were 2.40, 1.41, 0.922, and 2.65 ng As/ml, respectively, using the present HPLC–ICP MS method. NIES CRM No. 18 Human Urine (NIES, Tsukuba, Japan) was used as the standard reference material (SRM).

Statistics

Statistical analyses of data were performed using Student's *t*-test, with *P* values less than 0.05 considered significant.

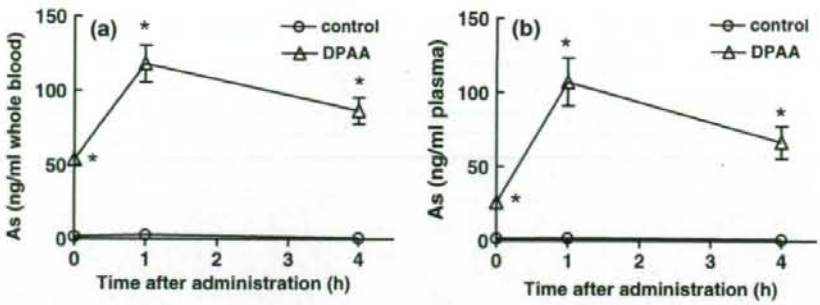

Fig. 2 Time courses of change in concentration of arsenic in **a** whole blood and **b** plasma after administration of DPAA or vehicle water (control) in pregnant cynomolgus monkeys. Values are the mean ± SEM ($n = 3$ for the control group and $n = 6$ for the DPAA group). *Asterisks* significantly increased compared to the control value

Results

Figure 2 shows the concentrations of arsenic in whole blood (Fig. 2a) and plasma (Fig. 2b) at 41–92 days after repeated administration of DPAA (1.0 mg/(kg day), twice daily) (Days 41–92). The blood was obtained just before and 1 and 4 h after administration. The vertical axis on the graph indicates the total concentration of arsenic, while the horizontal axis indicates elapsed time from the first administration of DPAA on the day of blood collecting. Compared to the DPAA group, only small amounts of arsenic were found in the control group (1.65 ± 0.509 ng As/ml in whole blood, and 1.39 ± 0.474 ng As/ml in plasma). The arsenic concentration in erythrocytes, calculated based on the reference hematocrit, was 2.04 ± 0.665 ng As/ml. Accordingly, approximately 50% of arsenic in whole blood was present in plasma and 50% in erythrocytes in the control group. On the other hand, in the DPAA group, arsenic concentration in whole blood was 53.4 ± 2.45 ng As/ml while that in plasma was 25.6 ± 1.90 ng As/ml. The arsenic concentration in erythrocytes was calculated to be 96.4 ± 3.90 ng As/ml, and accounted for 71% of whole blood arsenic, indicating that DPAA mainly accumulated in erythrocytes. Arsenic concentrations in whole blood were 117 ± 12.3 and 86.6 ± 9.05 ng As/ml 1 and 4 h after the first administration of DPAA, respectively. Subtracting the 0 h value (53.4 ± 2.45 ng As/ml) from the 1 and 4 h values, it was found that respectively 5.4 and 4.0% of the single dose of DPAA (0.14 mg As/kg) remained in whole blood 1 and 4 h after the first administration of DPAA.

Figure 3 shows concentrations of arsenic in the urine (Fig. 3a), feces (Fig. 3b), and hair (Fig. 3c) on Days 64–92 of administration of DPAA or vehicle water. The concentration of arsenic in 24 h-urine was 0.0287 ± 0.00440 μg As/ml in the control group and 2.28 ± 0.215 μg As/ml in the DPAA group (Fig. 3a). The daily arsenic excretion calculated using the quantity of collected urine was

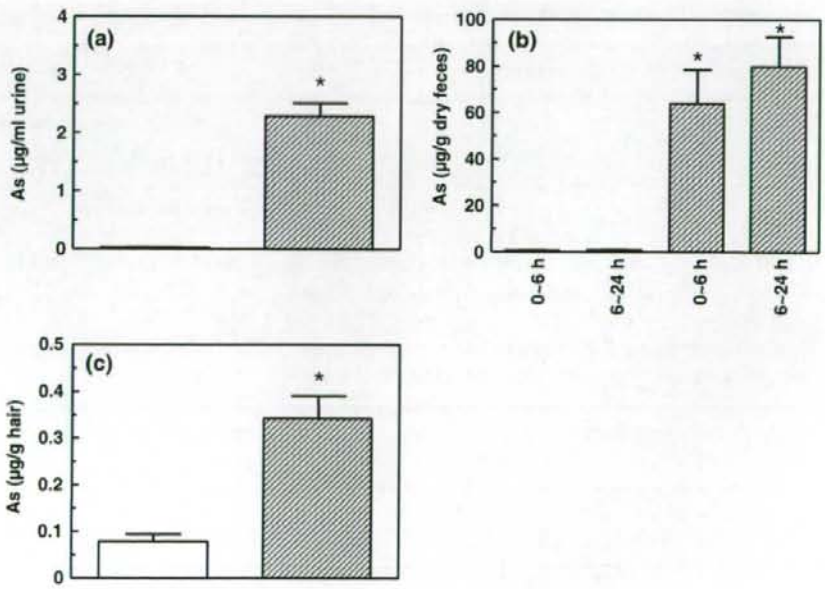

Fig. 3 Concentrations of arsenic in **a** urine, **b** feces, and **c** hair in pregnant cynomolgus monkeys subjected to repeated administration of DPAA or vehicle water. *Open columns* control group; *cross-hatched columns* DPAA group. Values are the mean ± SEM [$n = 3$ for the control group and $n = 5$ or 6 for the DPAA group ($n = 5$ for feces and $n = 6$ for urine and hair)]. *Asterisks* significantly increased compared to the control value

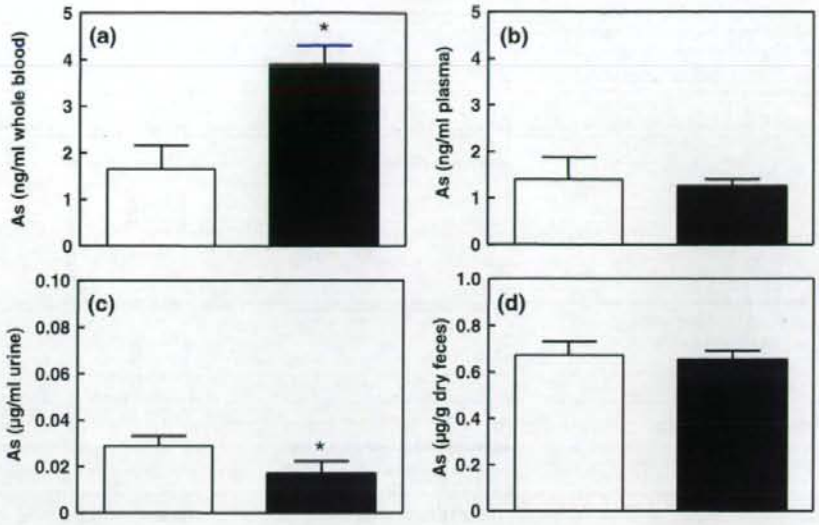

Fig. 4 Concentrations of arsenic in **a** whole blood, **b** plasma, **c** urine, and **d** feces in pregnant cynomolgus monkey 198–237 days after cessation of repeated administration of DPAA (recovery group). *Open columns* control group; *closed columns* recovery group. Values are the mean ± SEM ($n = 3$ for the control group and $n = 6$ for the recovery group). *Asterisks* significantly different from the control value

4.82 ± 1.84 μg in the control group and 395 ± 26.5 μg in the DPAA group. The concentration of arsenic in the feces was measured separately for 0–6 h (just after the first administration until the second administration) and 6–24 h periods (just after the second administration to the first administration on the following day). These values were 0.671 ± 0.0586 and 0.778 ± 0.0427 μg As/g in the control group and 63.7 ± 14.6 and 79.6 ± 13.0 μg As/g in the DPAA group (Fig. 3b). The daily excretion of arsenic was 5.54 ± 1.68 μg As in the control group and 616.9 ± 61.2 μg As in the DPAA group. Due to repeated administration of DPAA, the arsenic concentration in the hair of the DPAA group was approximately five times the control value (control group: 0.0786 ± 0.0153 μg As/g, DPAA group: 0.341 ± 0.0484 μg As/g) (Fig. 3c).

Figure 4 shows concentrations of arsenic in whole blood (Fig. 4a), plasma (Fig. 4b), 6-h urine (Fig. 4c), and 6-h feces (Fig. 4d) in the recovery group at 198–237 days after delivery (after cessation of repeated administration). At 198–237 days after cessation of administration, concentrations of arsenic were 3.89 ± 0.402 μg As/ml in whole blood (Fig. 4a), 1.25 ± 0.137 μg As/ml in plasma (Fig. 4b), and 7.96 ± 1.02 μg As/ml in erythrocytes. The concentrations of arsenic in plasma did not differ between the control and recovery groups, while there was a significant difference between these two groups in arsenic concentration in whole blood even 198–237 days after cessation of administration. Approximately 20% of whole blood arsenic was present in plasma and 80% in erythrocytes. The concentrations of arsenic in the urine (Fig. 4c) and feces (Fig. 4d) were 0.0169 ± 0.00597 μg As/ml and 0.653 ± 0.037 μg As/g, respectively, showing that fecal arsenic concentrations did not differ from those in the control group.

Figure 5a shows an elution profile of a standard solution containing DMA^V, AsB, and DPAA at concentrations of 10 ng As/ml. The elution profile of MMA^V is shown separately, since the retention time of MMA^V was close to that

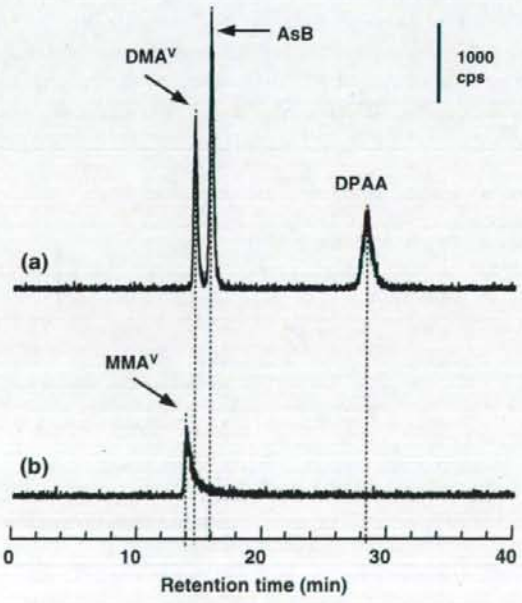

Fig. 5 Elution profiles of authentic arsenicals on a gel filtration column. Concentrations of arsenic in the eluate were measured by HPLC–ICP MS. A 20 μl aliquot of authentic arsenicals (10 ng As/ml each for DMA^V, AsB, DPAA and MMA^V) was applied to the column. The *vertical bars* indicate the level of detection at 1,000 counts per second

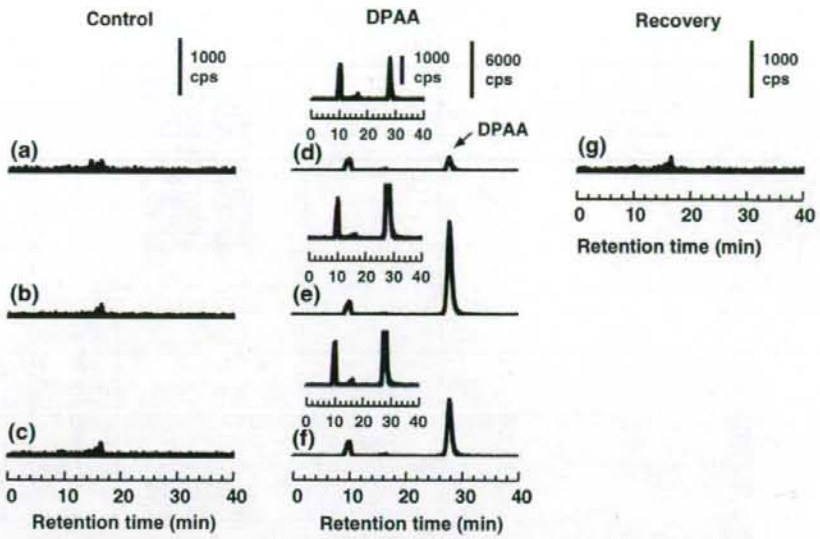

Fig. 6 Elution profiles of arsenicals in plasma on a gel filtration column. For arsenic speciation analyses, equal amounts of samples from the same group were combined. A 20 µl aliquot of sample was applied to the column. **a**–**c** Control group. **d**–**f** DPAA group. **g** Recovery group. The blood samples from the control and DPAA groups were collected before the first administration on the collection day (**a**, **d**) and 1 h (**b**, **e**), and 4 h (**c**, **f**) after the first administration of vehicle water or DPAA. The *vertical bars* indicate the level of detection at 1,000 and 6,000 counts per second

of DMA^V (Fig. 5b). MMA^V, DMA^V, AsB, and DPAA were eluted in this order using the present method of speciation.

The arsenic compounds in plasma from the control group were not detected as clear peaks (Fig. 6a–c). However, two arsenic peaks were observed in the plasma obtained on Days 41–92; one at the void volume appeared to be protein-bound arsenicals, while the other appeared at the same retention time as that of authentic DPAA (Fig. 6d–f). The peak height of the protein-bound arsenicals was unchanged at the following times: before (Fig. 6d), 1 h after (Fig. 6e), and 4 h after (Fig. 6f) the administration of DPAA. DPAA was present in plasma even 18 h after the second administration of DPAA on the preceding day (Fig. 6d). When 198–237 days had elapsed after cessation of administration, the elution profile of arsenic in plasma on the gel filtration column was almost the same as that in the control group (Fig. 6a, g).

The elution profiles of arsenic in the erythrocyte lysate were similar to those in the plasma (Fig. 7). Although the concentration of protein-bound arsenic in plasma had not changed over time (Fig. 6d–f), the peak of protein-bound arsenic in erythrocyte lysate increased 1 h after administration, and decreased to almost the same concentration as before administration (Fig. 7d–f).

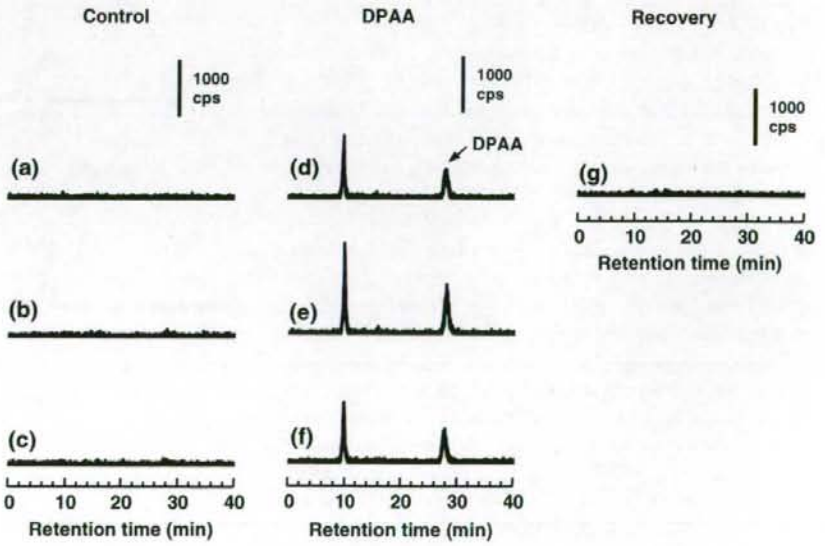

Fig. 7 Elution profiles of arsenicals in erythrocyte lysate on a gel filtration column. See also the legend to Fig. 6

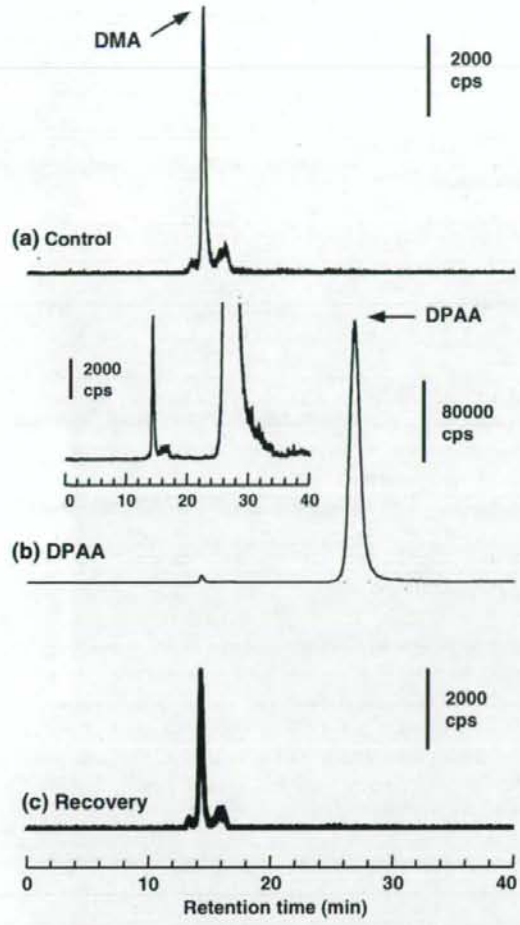

Fig. 8 Elution profiles of arsenicals in urine on a gel filtration column. For arsenic speciation analyses, equal amounts of each sample were combined. A 20 µl aliquot of sample was applied to the column. **a** Control group. **b** DPAA group. **c** Recovery group. The *vertical bars* indicate the level of detection at 2,000 and 80,000 counts per second

The major urinary metabolite in the control urine was DMA^V (Fig. 8a), while the major urinary arsenic during repeated administration of DPAA were unbound DPAA (Fig. 8b). DPAA was not detected in urine at 198–237 days after cessation of repeated administration, and DMA^V was again detected as the main arsenic compound in the recovery group (Fig. 8c).

The same samples as shown in Fig. 6a, d and g and Fig. 7a, d and g were heat-treated and centrifuged. The protein-rich pellet was treated with hydrogen peroxide to extract protein-bound arsenicals. Figure 9A and B show the elution profiles of arsenic in the extracted solution obtained from plasma and erythrocytes, respectively. The insets in Fig. 9 show the elution profiles of the supernatant of heat-treated samples without H_2O_2 treatment (Fig. 9Ab′, Bb′). Protein-bound peaks disappeared and only unbound DPAA was detected in the heat- and H_2O_2-treated plasma and erythrocyte lysate obtained from the DPAA group (Fig. 9Ab, Bb). No extractable DPAA was detected in the recovery group (Fig. 9Ac, Bc).

We also examined the stability of protein-bound DPAA compounds in erythrocyte lysate. When the samples were incubated at 37°C for 0–24 h, the peak representing the protein-bound arsenic decreased over time, while the unbound DPAA peak increased slightly (Fig. 10).

Discussion

Diphenylarsinic acid is a product of degradation as well as a reagent used for the synthesis of the CWAs Clark 1 and Clark 2. Although DPAA does not occur naturally, its chemical form is similar to DMA^V, a major metabolite of inorganic arsenicals and a well-known worldwide pollutant in drinking water and coal (Crecelius 1977; Smith et al. 1977; IPCS 1981, 2001). In the present study, we examined the distribution and excretion of repetitively administered DPAA in cynomolgus monkeys.

Arsenic accumulated in blood and hair during repeated administration of DPAA (Figs. 2, 3c). Daily excretion of DPAA was approximately 40% in urine and 60% in feces (Fig. 3a, b). With repeated administration of DPAA, a high level of arsenic was detected in whole blood, with 71% of arsenic distributed to the erythrocytes. It has been shown that dimethylarsenic compounds accumulated in rat erythrocytes (Lerman and Clarkson 1983; Vahter et al. 1984; Shiobara et al. 2001). In the present study DPAA was also found to be accumulated in the erythrocytes of cynomolgus monkeys. Notably, arsenic concentration in whole blood in the recovery group was significantly higher than the control value even 198–237 days after cessation of administration (Fig. 4a). Although the concentration of arsenic in plasma did not differ between the control and recovery groups, the proportions of arsenic in erythrocytes were approximately 50 and 80 % in the control and recovery groups, respectively. These findings suggested that arsenic was still present in the erythrocytes of monkeys even 198–237 days after cessation of administration (Fig. 4a), although the arsenic compounds obtained from the recovery group were not detected as clear peaks by HPLC–ICP MS (Fig. 7g).

Both protein-bound and unbound DPAA were detected when chemical speciation of arsenic in plasma and erythrocyte lysate was performed by HPLC–ICP MS (Figs. 6d, 7d). DPAA was released from protein-bound arsenic compounds after treatment with hydrogen peroxide (Fig. 9Ab, Bb). Lu et al. (2004) reported that arsenic was found as protein-bound compounds in the erythrocytes of rats that had

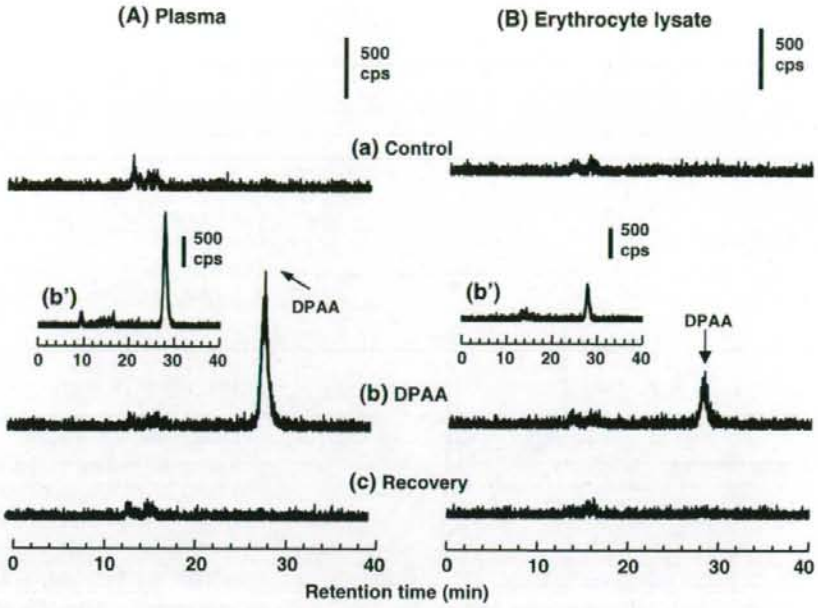

Fig. 9 Elution profiles of arsenicals in H_2O_2-treated plasma and erythrocyte lysate on a gel filtration column. A 20 µl aliquot of sample was applied to the column. **a** Control group. **b** DPAA group. **c** Recovery group. **b'** *Insets* for the DPAA group indicate elution profiles of arsenicals in blood samples of the DPAA group without H_2O_2 treatment (heat treatment alone). The *vertical bars* indicate the level of detection at 500 counts per second

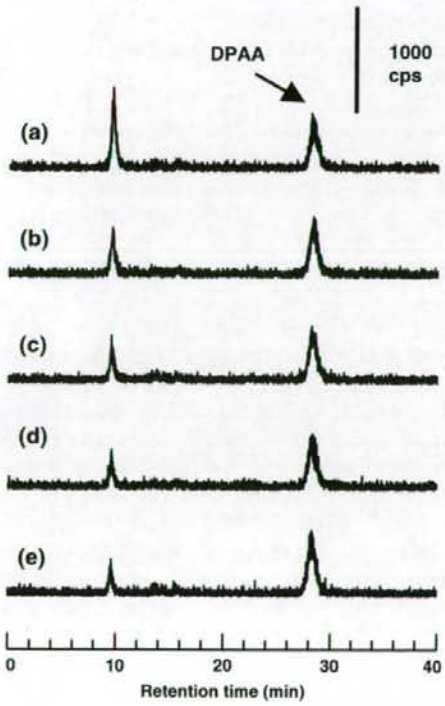

Fig. 10 Effects of incubation time on the stability of protein-bound arsenicals in erythrocyte lysate. Erythrocyte lysate samples obtained from DPAA-treated cynomolgus monkeys (corresponding to Fig. 7d) were incubated at 37°C for **a** 0, **b** 1, **c** 3, **d** 6, and **e** 24 h. The vertical bars indicate the level of detection at 1000 counts per second

been fed a DMA^V-containing diet. Chemical analysis using nanoelectrospray mass spectrometry also indicated that the main arsenical in erythrocyte was dimethylarsinous acid (DMA^{III}), bound to the hemoglobin α-unit (Lu et al. 2004). Taken together, these findings suggest that the protein-bound arsenic compound found in the present study was probably a trivalent diphenylarsenical. In the plasma of the DPAA group, the DPAA peak transiently increased after 1 h and then decreased after 4 h. However, the peak of protein-bound arsenic compounds was unchanged (Fig. 6d–f). Our findings indicate that the increase in arsenic concentration in plasma shown in Fig. 2b was due to unbound DPAA. On the other hand, in erythrocyte lysate, the peak of protein-bound arsenic compounds increased at 1 h post-administration and decreased thereafter (Fig. 7d–f). These findings suggested that DPAA was rapidly absorbed into erythrocytes. In aerobic condition, the protein-bound arsenic compounds were not stable, since the corresponding peak decreased over time with incubation at 37°C (Fig. 10). Thus, unbound DPAA, which was detected in plasma (Fig. 6d–f) and erythrocyte lysate (Fig. 7d–f) in the DPAA group, may have been released at least in part from protein-bound DPAA after oxidization. The concentrations of arsenic in plasma, urine, and feces 198–237 days after termination of repeated administration decreased to the same level as in the control group (Fig. 4). In light of the fact that the lifespan of monkey erythrocytes is 86–105 days (Tanimoto 1982), it appears that DPAA accumulated in the erythrocytes as protein-bound trivalent DPAA and was slowly released as unbound DPAA, although the arsenic

concentration in erythrocytes was still higher than the control value even 198–237 days after cessation of administration.

Acknowledgments We would like to thank the staff of Shin Nippon Biomedical Laboratories, Ltd. for completion of the animal experiments. The present research was funded by the Ministry of the Environment of Japan, and submission of the manuscript has been approved by the Ministry. Approval of submission does not signify that the contents of the manuscript necessarily reflect the views of the Ministry.

References

Aposhian HV (1997) Enzymatic methylation of arsenic species and other new approaches to arsenic toxicity. Annu Rev Pharmacol Toxicol 37:397–419

Crecelius EA (1977) Changes in the chemical speciation of arsenic following ingestion by man. Environ Health Perspect 19:147–150

Hirano S, Kobayashi Y, Hayakawa T, Cui X, Yamamoto M, Kanno S, Shraim A (2005) Accumulation and toxicity of monophenyl arsenicals in rat endothelial cells. Arch Toxicol 79:54–61

IPCS (1981) Arsenic. World Health Organization, Geneva

IPCS (2001) Arsenic and arsenic compounds. World Health Organization, Geneva

Ishii K, Tamaoka A, Otsuka F, Iwasaki N, Shin K, Matsui A, Endo G, Kumagai Y, Ishii T, Shoji S, Ogata T, Ishizaki M, Doi M, Shimojo N (2004) Diphenylarsinic acid poisoning from chemical weapons in Kamisu, Japan. Ann Neurol 56:741–745

Kinoshita K, Shida Y, Sakuma C, Ishizaki M, Kiso K, Shikino O, Ito H, Morita M, Ochi T, Kaise T (2005) Determination of diphenylarsinic acid and phenylarsonic acid, the degradation products of organoarsenic chemical warfare agents, in well water by HPLC-ICP-MS. Appl Organomet Chem 19:287–293

Lerman S, Clarkson TW (1983) The Metabolism of Arsenite and Arsenate by the Rat. Fundam Appl Toxicol 3:309–314

Lu M, Wang H, Li XF, Lu X, Cullen WR, Arnold LL, Cohen SM, Le XC (2004) Evidence of hemoglobin binding to arsenic as a basis for the accumulation of arsenic in rat blood. Chem Res Toxicol 17:1733–1742

Ochi T, Suzuki T, Isono H, Kaise T (2004) In vitro cytotoxic and genotoxic effects of diphenylarsinic acid, a degradation product of chemical warfare agents. Toxicol Appl Pharmacol 200:64–72

Ochi T, Kinoshita K, Suzuki T, Miyazaki K, Noguchi A, Kaise T (2006) The role of glutathione on the cytotoxic effects and cellular uptake of diphenylarsinic acid, a degradation product of chemical warfare agents. Arch Toxicol 80:486–491

Shibata Y, Tsuzuku K, Komori S, Umedzu C, Imai H, Morita M (2005) Analysis of diphenylarsinic acid in human and environmental samples by HPLC-ICP-MS. Appl Organomet Chem 19:276–281

Shiobara Y, Ogra Y, Suzuki KT (2001) Animal species difference in the uptake of dimethylarsinous acid (DMA(III)) by red blood cells. Chem Res Toxicol 14:1446–1452

Shraim A, Cui X, Li S, Ng JC, Wang HP, Jin YL, Liu YC, Guo L, Li DS, Wang SQ, Zhang RZ, Hirano S (2003) Arsenic speciation in the urine and hair of individuals exposed to airborne arsenic through coal-burning in Guizhou, PR China. Toxicol Lett 137:35–48

Smith TJ, Crecelius EA, Reading JC (1977) Airborne arsenic exposure and excretion of methylated arsenic compounds. Environ Health Perspect 19:89–93

Tanimoto Y (1982) Hematology-human and animal's points of contact. Seishi Shoin, Tokyo (in Japanese)

Vahter M, Marafante E, Dencker L (1984) Tissue distribution and retention of 74As-dimethylarsinic acid in mice and rats. Arch Environ Contam Toxicol 13:259–264

Yoshida T, Fujimoto K (2006) Cynomolgus monkey as medical science study research resource. Springer, Tokyo (in Japanese)

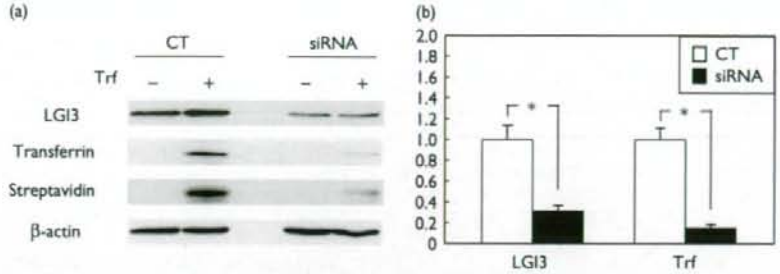

Fig. 3 (a) Western blots showing the amount of leucine-rich glioma inactivated 3 (LGI3) and the uptake levels of transferrin (Trf) in Neuro2a cells 72 h after treatment with siRNA-I. In cells transfected with siRNA-I, LGI3 was clearly downregulated, and the uptake level of transferrin apparently decreased. (b) Histograms showing the effect of siRNA-I transfection on the amount of LGI3-fl and on the uptake level of transferrin in Neuro2a cells. All data were normalized according to β-actin protein levels (CT, control). Values are means ± SD. $^*P < 0.001$. CT, cells transfected with control siRNA; siRNA, cells transfected with siRNA-I. Y-axes show the mean values of the quantified data.

that LGI3 colocalized with lipid raft markers in monkey brains [9], LGI3 indeed may play a role not only in the clathrin-dependent endocytosis but also in other types of systems such as the lipid raft-mediated endocytosis.

Furthermore, the downregulation of LGI3 also significantly decreased transferrin uptake by neuronal cell line, Neuro2a (Fig. 3). This result is consistent with our earlier finding that LGI3 colocalized with endocytosis-associated proteins even in neurons of monkey brains [9], suggesting that LGI3 would be involved in endocytosis in neurons as well as astrocytes. Endocytosis is considered to be required for Aβ processing from amyloid precursor protein [13]. Although additional investigations are needed to clarify whether LGI3 mediates amyloid precursor protein endocytosis and its processing in neurons, the results of this study support our hypothesis that LGI3 is involved in Aβ uptake by astrocytes and even endocytosis itself.

Conclusion

LGI3 is localized to the endocytic pathway, and siRNA studies demonstrated that LGI3 is involved in endocytosis in neural cells. Although additional investigations are needed to determine the precise function of LGI3, this line of research will reveal details of the endocytosis system in the brain and its relationship to Aβ pathology.

Acknowledgements

Authors thank Dr T. Yoshida and D. Y. Yokota for neuronal cell line, Neuro2a.

This study was supported by a grant-in-aid for Young Scientists (B) from the Ministry of Education, Culture, Sports, Science and Technology, Japan (18790288).

References

1. Glenner GG. Alzheimer's disease: its proteins and genes. *Cell* 1988; **2**: 307–308.
2. Glenner GG. The proteins and genes of Alzheimer's disease. *Biomed Pharmacother* 1988; **42**:579–854.
3. Younkin SG. The amyloid beta protein precursor mutations linked to familial Alzheimer's disease alter processing in a way that fosters amyloid deposition. *Tohoku J Exp Med* 1994; **174**:217–223.
4. Mattson MP. Pathways towards and away from Alzheimer's disease. *Nature* 2004; **30**:631–639.
5. Funato H, Yoshimura M, Yamazaki T, Saido TC, Ito Y, Yokohujita J, *et al.* Astrocytes containing amyloid beta-protein (Abeta)-positive granules are associated with Abeta40-positive diffuse plaques in the aged human brain. *Am J Pathol* 1998; **152**:983–992.
6. Matsunaga W, Shirokawa T, Isobe K. Specific uptake of Aβ 1-40 in rat brain occurs in astrocyte, but not in microglia. *Neurosci Lett* 2003; **342**: 129–131.
7. Wyss-Coray T, Loike JD, Brionne TC, Lu E, Anankov R, Yan F, *et al.* Adult mouse astrocytes degrade amyloid-β in vitro and in situ. *Nat Med* 2003; **9**:453–457.
8. Kimura N, Ishii Y, Suzaki S, Negishi T, Kyuwa S, Yoshikawa Y. Aβ upregulates and colocalizes with LGI3 in rat cultured astrocytes. *Cell Mol Neurobiol* 2007; **27**:335–350.
9. Okabayashi S, Kimura N. Immunohistochemical and biochemical analyses of LGI3 in monkey brain: LGI3 accumulates in aged monkey brains. *Cell Mol Neurobiol* 2007; **27**:819–830.
10. Negishi T, Ishii Y, Kyuwa S, Kuroda Y, Yoshikawa Y. Primary culture of cortical neurons, type-1 astrocytes, and microglial cells from cynomolgus monkey (*Macaca fascicularis*) fetuses. *J Neurosci Method* 2003; **131**:33–140.
11. Ida N, Hartmann T, Pantel J, Schröder J, Zerfass R, Förstl H, *et al.* Analysis of heterogeneous A4 peptides in human cerebrospinal fluid and blood by a newly developed sensitive western blot assay. *J Biol Chem* 1996; **271**:22908–22914.
12. Saavedra L, Mohamed A, Ma V, Kar S, De Chaves EP. Internalization of beta-amyloid peptide by primary neurons in the absence of apolipoprotein E. *J Biol Chem* 2007; **282**:35722–35732.
13. Small SA, Gandy S. Sorting through the cell biology of Alzheimer's disease: intracellular pathways to pathogenesis. *Neuron* 2006; **52**:15–31.